Adsorption 6, 137–147, 2000


# Why Does the Linear Driving Force Model for Adsorption Kinetics Work?

S. SIRCAR* AND J.R. HUFTON
*Air Products and Chemicals, Inc., 7201 Hamilton Boulevard, Allentown, PA 18195-1501, USA*

*Received August 26, 1999; Revised January 25, 2000; Accepted February 7, 2000*

**Abstract.** The Linear Driving Force (LDF) model for gas adsorption kinetics is frequently and successfully used for analysis of adsorption column dynamic data and for adsorptive process designs because it is simple, analytic, and physically consistent. Yet, there is a substantial difference in the characteristics of isothermal batch uptake curves on adsorbent particles by the LDF and the more rigorous Fickian Diffusion (FD) model. It is demonstrated by using simple model systems that the characteristics of the adsorption kinetics at the single pore or the adsorbent particle level are lost in (a) evaluating overall uptake on a heterogeneous porous solid, (b) calculating breakthrough curves from a packed adsorbent column, and (c) establishing the efficiency of separation by an adsorptive process due to repeated averaging of the base kinetic property. That is why the LDF model works in practice.

**Keywords:** adsorption, kinetics, linear driving force model, process design

## Introduction

Mathematical simulation of cyclic gas separation processes such as pressure swing adsorption or thermal swing adsorption (PSA or TSA) requires models for describing adsorption kinetics. The linear driving force (LDF) model, which was originally proposed by Gleuckauf and Coates (1947) for adsorption chromatography, is frequently used for this purpose because it is analytical, simple, and physically consistent (Hartzog and Sircar, 1995; Gemmingen, 1993; Raghavan et al., 1986; Chihara and Suzuki, 1983).

According to the LDF model, the rate of adsorption of a single adsorbate (pure gas or mixture with an inert gas) into an adsorbent particle is given by:

$$\frac{d\bar{C}(t)}{dt} = k_{\mathrm{L}}[\bar{C}^*(t) - \bar{C}(t)] \qquad (1)$$

where $\bar{C}(t)$ is the average adsorbate concentration (moles per unit volume) in the adsorbent particle at time $t$, and $\bar{C}^*(t)$ is the adsorbate concentration in the particle that would be in equilibrium with the instantaneous superincumbent gas phase partial pressure of the adsorbate $[P(t)]$ and the adsorbent temperature $[T(t)]$ at time $t$. The model assumes that the adsorbent particle temperature is uniform (does not vary with radius) at all times. The variable $k_{\mathrm{L}}$ is called the effective LDF mass transfer coefficient at adsorbate loading of $(\bar{C})$ and temperature $(T)$. The average adsorbate loading (moles per unit weight) at time $t$ is given by $\bar{n}(t) = \bar{C}(t)/\rho_{\mathrm{P}}$, where $\rho_{\mathrm{P}}$ is the adsorbent particle density.

The most rigorous formulation to describe adsorbate transport inside the adsorbent particle is the chemical potential driving force (CPDF) model which originates from the irreversible thermodynamics (Barrer, 1971). For pure gas ad(de)sorption into (from) a spherical adsorbent particle of radius $(R)$, the CPDF model yields:

$$J(r,t) = -B \cdot C(r,t)\left[\frac{\partial\{\mu(r,t)/R_{\mathrm{g}}T\}}{\partial r}\right]_t \qquad (2)$$

where $J(r,t)$ is the flux of a pure adsorbate (moles per unit area per time) at radius $r\,(0 \le r < R)$ of the adsorbent particle at time $t$ where the instantaneous local adsorbate concentration is $C(r,t)$ and the instantaneous local temperature is $T(r,t)$. The variable $B$ is called the mobility of the adsorbate at $C$ and $T$, and $R_{\mathrm{g}}$ is the gas constant. The instantaneous local chemical potential $[\mu(r,t)]$ of the pure adsorbate inside the

*Author to whom correspondence should be addressed.

adsorbent at $r$ and $t$ is given by:

$$\mu(r,t) = \mu^*(T) + R_g T \ln P(r,t) \tag{3}$$

where $\mu^*(T)$ is the standard state gas phase chemical potential of the pure adsorbate at temperature $T$ (pressure = one atmosphere), and $P(r,t)$ is the pure gas partial pressure which will be in equilibrium with the particle adsorbate concentration of $C(r,t)$.

For the special case of isothermal ad(de)sorption process at temperature $T$, Eqs. (2) and (3) can be combined to obtain:

$$J(r,t) = -D \cdot \left(\frac{\partial C}{\partial r}\right)_t \quad \text{constant } T \tag{4}$$

$$D = B\left[\frac{d \ln P}{d \ln C}\right]_T \tag{5}$$

Equation (4) is the well-known isothermal Fickian diffusion (FD) model for isothermal pure gas ad(de)sorption. The parameter $D$ is called the Fickian diffusivity. Equation (5) is known as the "Darken correction" (Karger and Ruthven, 1992), which relates the parameters $B$ and $D$. The quantity $[\frac{d \ln P}{d \ln C}]_T$ in Eq. (5) is the inverse of the slope of the equilibrium adsorption isotherm of the pure gas (plotted as $\ln C$ vs. $\ln P$).

For the special case of isothermal adsorption at low gas pressures (Henry's law region), where the adsorption isotherms are linear [$C = KP$], the FD model further simplifies to

$$J(r,t) = -D^0 \cdot \left(\frac{\partial C}{\partial r}\right)_t \tag{6}$$

where $D^0(=B)$ is the Henry's law region diffusivity for pure gas adsorption and $K$ is the Henry's law constant.

It is generally assumed that $D^0$ is a function of $T$ only. Thus, the local isothermal adsorbate mass balance within the adsorbent particle at radius $r$ and time $t$ can be written as:

$$\left[\frac{\partial C(r,t)}{\partial t}\right]_r = \frac{D^0}{r^2} \cdot \frac{\partial}{\partial r}\left[r^2 \cdot \left(\frac{\partial C}{\partial r}\right)_t\right]_t \tag{7}$$

The average adsorbate concentration in the particle at time $t[\bar{C}(t)]$ is given by

$$\bar{C}(t) = \frac{3}{R^3}\int_0^R r^2 C(r,t)\, dr \tag{8}$$

Many analytical solutions for Eqs. (7) and (8) have been generated [isothermal ad(de)sorption with constant $D^0$] by using different initial and boundary conditions for the batch uptake experiments (Crank, 1956). They are expressed in terms of the fractional uptakes (loss) of the adsorbate [$f(t)$] as functions of the dimensionless times ($\tau = D^0 t/R^2$], which is defined by:

$$f(t) = \frac{\bar{C}(t) - \bar{C}^0}{\bar{C}^\infty - \bar{C}^0}$$

where $\bar{C}^0$ and $\bar{C}^\infty$ are, respectively, the initial and final equilibrium adsorbate concentrations in the adsorbent particle at the start and end of the batch uptake (loss) experiment. The corresponding equilibrium gas phase adsorbate partial pressures are $P^0$ and $P^\infty$, respectively.

Table 1 reproduces the analytical expressions for $f(t)$ obtained under isothermal, constant volume and constant pressure experiments for the FD model. The

*Table 1.* Analytical batch uptake curves.

| Models | Constant pressure experiment | Constant volume experiment |
|---|---|---|
| Fickian Diffusion (FD) | $f(t) = 1 - \sum_{n=1}^{\infty} \frac{6}{(n\pi)^2} e^{-[Dn^2\pi^2 t/R^2]}$ | $f(t) = 1 - \sum_{n=1}^{\infty} \frac{6\alpha(1+\alpha)e^{-[Dq_n^2 t/R^2]}}{(9+9\alpha+q_n^2\alpha^2)}$ |
| | | $\tan q_n = \frac{3q_n}{3+\alpha q_n^2}$ |
| Linear Driving Force (LDF) | $f(t) = 1 - e^{-k_L t}$ | $f(t) = 1 - e^{-\frac{(1+\alpha)}{\alpha} k_L t}$ |
| Quadratic Driving Force (QDF) | $\ln[1 - f(t)] + \ln\left[1 + \frac{f}{(1+2\beta)}\right] = -k_Q t$ | $\ln[1 - f(t)] + \frac{(\alpha+1)}{(\alpha-1)} \ln\left[1 + \frac{f}{\delta}\right]$ |
| | $\beta = \frac{\bar{C}^0}{(\bar{C}^\infty - \bar{C}^0)}$ | $= -\frac{(1+\alpha)}{\alpha} k_Q t$ |
| | | $\delta = \frac{(1+\alpha+2\alpha\beta)}{(\alpha-1)}$ |
| | | $\beta = \bar{C}^0/(\bar{C}^\infty - \bar{C}^0)$ |
| | Special case $\beta = 0$ | Special case $\beta \to \infty$ |
| | $f^2(t) = 1 - e^{-k_Q t}$ | $f(t) = 1 - e^{-\frac{(1+\alpha)}{\alpha} k_Q t}$ |

gas phase pressure is instantaneously changed from $P^0$ to $P^{**}$ at $t = 0$, and then it gradually approaches $P^\infty$ ($t \to \infty$) during the constant volume experiment (volumetric apparatus). The gas phase pressure is instantaneously changed from $P^0$ to $P^\infty$ at $t = 0$, and then it is held constant at that value during the constant pressure experiment (gravimetric apparatus). An additional parameter ($\alpha$) is needed to describe the uptake by the constant volume experiment. The quantity $[1/(1 + \alpha)]$ represents the fraction of moles of adsorbate introduced (removed) into (from) the gas phase of the ad(de)sorption system at $t = 0$ (in order to raise (lower) the gas phase pressure from $P^0$ to $P^{**}$) that is ad(de)sorbed during the process. The constant pressure experiment represents a special case of the constant volume experiment where $\alpha \to \infty$.

The solutions of Table 1 are frequently used to obtain $D^0$ from the experimental volumetric or gravimetric uptake data. It should, however, be emphasized that these solutions are rigorously applicable only for isothermal uptakes and for the case where $D$ is not a function of $C$. Otherwise, the calculated values of diffusivity will be erroneous even though the model may fit the data fairly well. Recently conducted uptake studies using the isotope exchange technique (Rynders et al., 1997; Mohr et al., 1999), where the process is truly isothermal and the effective adsorption isotherms for the isotopes are linear, showed that the FD models describe the process very well for diffusion of simple gases in zeolites. Other non-isothermal FD models, which simultaneously solve mass and heat balance equations for the differential uptake process have also been used to demonstrate the validity of the FD model (Yucel and Ruthven, 1980; Ruthven et al., 1980).

It is generally assumed that the FD model is fundamentally adequate to describe pure gas ad(de)sorption kinetics. However, the model imposes formidable mathematical hurdles in adsorptive process design because (a) Eqs. (4) and (5) have to be integrated at the adsorbent particle level under the local operating conditions of the process in order to obtain the distributed adsorbate loadings $[\bar{n}(t, z)]$ as functions of time ($t$) and adsorbent particle position ($z$) within a packed-column adsorber during each cyclic step of the process, (b) the $\bar{n}(t, z)$ profiles must then be integrated over the column length ($L$) and step cycle times ($t^s$) in order to obtain the average column adsorbate loadings at the start and the end of various cyclic steps of the process, and finally (c) the above integration protocols must be repeated over many cycles of operation in order to establish the final cyclic-steady-state separation performance of the overall process. Since all practical adsorbers operate under non-isothermal and non-isobaric conditions, the above described integrations must be carried out by coupling the solutions of simultaneous mass, heat, and momentum balance equations at the particle, column, and steady state cyclic operation levels. As a result, the FD model will generally require impractically large computational times for process simulation under realistic conditions. The authors are not aware of any publication that uses such a model for adsorptive process design. On the other hand, the mathematically simple LDF model eliminates the integration step at the particle level and it significantly reduces the computational times required for realistic process simulations.

The purpose of the present work is to demonstrate that the LDF model is adequate for process simulation because the detailed characteristics of a local adsorption kinetic model are lost during repeated integrations (averaging) of its properties needed to obtain the final process performance.

## Comparison Between Batch Uptakes by FD and LDF models

Table 1 gives the analytical expressions for isothermal fractional uptakes $[f(t)]$ by the LDF kinetic model using the batch constant volume and the constant pressure experiments. The dimensionless time for the LDF model is defined by $\tau (= k_L t)$.

Curve (a) of Fig. 1 shows the characteristics of dimensionless uptake by the FD model for a constant pressure experiment. The best least square fit of curve

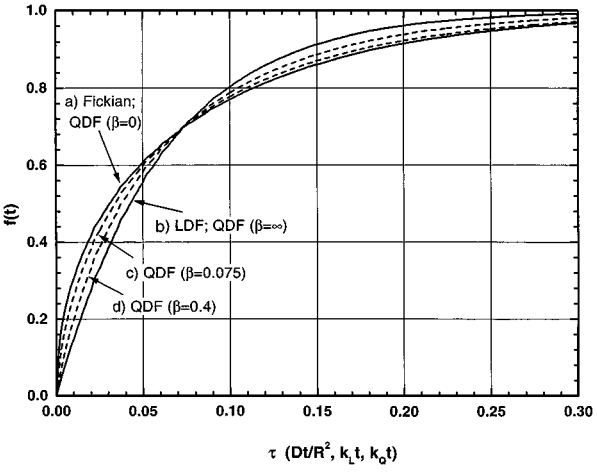


*Figure 1.* Comparative batch kinetic uptakes by FD, LDF, and QDF models (constant pressure experiment).

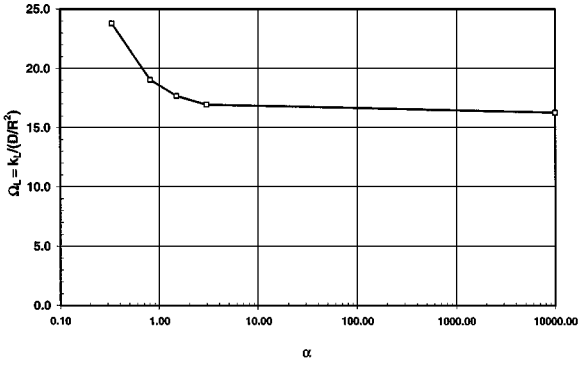


*Figure 2.* Best fit relationship between $k_L$ and $(D/R^2)$ for batch kinetic uptake (constant volume experiment).

(a) by the LDF model is shown by curve (b) of the figure. The LDF model underpredicts the value of $f(\tau)$ by the FD model at lower values of $t$ and overpredicts the $f(\tau)$ value at higher values of $t$. However, the general shapes of the uptake curves ($f$ vs $\tau$) by both models are similar.

The best fit relationship between the time constants for the adsorbate uptakes by the FD$(D/R^2)$ and the LDF ($k_L$) models for the constant pressure experiment of Fig. 1 is given by $[\Omega_L = k_L/(D/R^2) = 16.2]$. Similar best fit relationships can be generated to obtain $\Omega_L$ for constant volume experiments as functions of the parameter $\alpha$. Figure 2 shows the results. It may be seen that $\Omega_L$ is practically independent of $\alpha$ for larger values of $\alpha(\geq 5)$ and it increases ($>16$) as $\alpha$ decreases. The general discrepancies between the uptake curves for FD and LDF models obtained for constant volume experiments (finite $\alpha$) are very similar (not shown) to those for the constant pressure experiments.

It may be interesting to note that Glueckauf (1955) obtained a ratio of 15 for $\Omega_L$ by comparing theoretical chromatograms by the two models. It will be shown later that other relationships for $\Omega_L$ can be obtained by matching the net adsorbate flux into the adsorbent particle by the two models and assuming different adsorbate concentration profiles within the particle (same average concentration) for the LDF model. A special case of this latter approach, which assumes an intraparticle quadratic adsorbate concentration profile (Liaw et al., 1979), yields a value of 15 for $\Omega_L$ which is commonly recommended for process design (Ruthven, 1984).

The lack of quantitative fit between the batch kinetic uptake curves of Fig. 1 by the FD and the LDF models has led many workers to empirically modify the form of Eq. (1) in order to obtain better match with the FD uptake (Do and Rice, 1986; Do and Mayfield, 1987; Goto and Hirose, 1991; Buzanowski and Yang, 1991; Yao and Tien, 1992a, 1992b). These modified models, however, become mathematically cumbersome even for the simple case of isothermal ad(de)sorption and often contain several parameters which cannot be unambiguously evaluated from the experimental uptake data. Furthermore, the integrable characteristics of the LDF model, which is a very desirable property for the evaluation of adsorption column dynamics or process design, is often lost.

A better fit of the FD model uptake curve under certain conditions can be achieved by the Quadratic Driving Force (QDF) model (Vermeulen, 1953). The rate of adsorption into the adsorbent particle by this empirical model is given by

$$\frac{d[\bar{C}(t)]}{dt} = \frac{k_Q[\{\bar{C}^*(t)\}^2 - \{\bar{C}(t)\}^2]}{2\{\bar{C}(t)\}} \tag{9}$$

where $k_Q$ is the effective QDF mass transfer coefficient at adsorbate loading of $\bar{C}(t)$ and temperature $T$.

Table 1 gives the analytical solutions for the uptake curves generated by the QDF model. An additional parameter called $\beta$ $[=\bar{C}^0/(\bar{C}^\infty - \bar{C}^0)]$ is required to describe these solutions.

Figure 1 shows that the uptake curve by the QDF model for a constant pressure experiment ($\alpha \to \infty$) very closely traces that by the FD model when $\beta = 0$ ($\bar{C}^0 = 0$, adsorbent is initially free of adsorbate) even though the instantaneous rate of adsorption at the limit of $t = 0$ is undefined [Eq. (9)] by the model under that condition. This limiting singularity vanishes for finite values of $\beta$ but the difference between the uptake curves by the FD and the QDF models becomes more pronounced as $\beta$ increases (Fig. 1). The uptake curves for the QDF and the LDF models coincide when $\beta \to \infty$ (a differential uptake test where $\bar{C}^\infty \approx \bar{C}^0$).

Figure 3 compares the uptake curves for the FD and QDF models for a constant volume experiment ($\alpha =$ finite) with $\beta = 0$. It shows that these two models are practically indistinguishable over a very large value of $\alpha$ ($1 \leq \alpha \leq 10{,}000$) under this condition. The ratio of the least square best fit values of $k_Q$ and $(D/R^2)$ is given by 9.14 ($=\Omega_Q$) when $\alpha$ is large. The differences between these two models, however, become more pronounced (as in Fig. 1) when $\beta$ is large (not shown).

Thus, it may be concluded that the QDF model is a good proxy for describing isothermal Fickian uptake of a pure gas by an adsorbent particle when the initial adsorbate loading is small. We will utilize this characteristic of the QDF model to analytically represent Fickian mass transfer in adsorption columns in this paper.

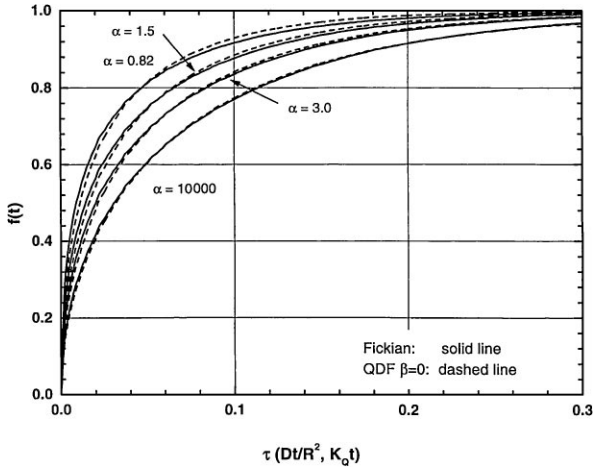


*Figure 3.* Comparative batch kinetic uptakes by FD and QDF models (constant volume experiment).

### Intraparticle Concentration Profile for LDF Model

Even though the rate equation for the LDF model Eq. (1) deals with the average adsorbate concentrations within the adsorbent particle, it has been shown (Sircar and Hufton, 2000) that the following very general intraparticle adsorbate concentration profile is compatible with that rate equation for a constant pressure experiment:

$$C(r,t) = \bar{C}^{\infty} - b(t) \cdot [F_R - F(r)] \tag{10}$$

$$b(t) = \frac{[\bar{C}^{\infty} - \bar{C}^{0}]}{F_R - G_R} e^{-k_L t} \tag{11}$$

$$G_R = \frac{3}{R^3} \int_0^R r^2 F(r)\, dr \tag{12}$$

where $F(r)$ is any monotonic and continuous function of $r$ in the domain ($0 \leq r \leq R$) which satisfies the boundary condition [$\frac{dF(r)}{dr} = 0$ at $r = 0$]. The value of the function $F(r)$ at $r = R$ is $F_R$.

The net instantaneous adsorbate flux into the adsorbent particle for the FD and LDF models can be written (constant pressure experiment) as:

$$\frac{d\bar{C}(t)}{dt} = k_L[\bar{C}^{\infty} - \bar{C}(t)] = \frac{3D}{R} \cdot \left[\frac{\partial C(r,t)}{\partial r}\right]_{r=R} \tag{13}$$

It follows from Eqs. (10)–(13) that

$$k_L = \frac{3D}{R} \frac{H_R}{[F_R - G_R]}; \quad \Omega_L = \frac{3RH_R}{[F_R - G_R]} \tag{14}$$

where $H_R$ is given by the value of [$\frac{dF(r)}{dr}$] at $r = R$.

Equation (14) provides a very general relationship between $k_L$ and $(D/R^2)$ which is obtained by matching the net instantaneous adsorbate flux into the adsorbent particles by the two models for a constant pressure experiment. Thus, the value of $\Omega_L$ depends on the choice of the function $F(r)$. The commonly used value of 15 is true only for the special case where

$$C(r,t) = \bar{C}^{\infty} - b(t)[R^2 - r^2] \tag{15}$$

Equation (15) was originally proposed by Liaw et al. (1979).

### Effect of Adsorbent Heterogeneity

The above discussions are based on the assumption that the adsorbent particle is physico-chemically homogenous so that a single value of $(D/R^2)$ or $k_L$ characterizes the mass transfer into the adsorbent. Most practical amorphous and bounded crystalline adsorbents are, however, heterogeneous consisting of a network of interconnected pores of different sizes and shapes and different surface chemistry. Quantitative estimation of such heterogeneity is not practically possible by today's technology. Consequently, the experimentally measured uptake profiles on these materials already reflect the average rate of adsorption by the composite pore structure of the adsorbent.

We evaluated the effect of this averaging by assuming that the model heterogeneous adsorbent consists of a collection of parallel pores, each having a different $k_L$ or $D$ value. A normalized gamma distribution function was assumed to represent the adsorbent heterogeneity. Thus, the average fractional uptake $[F(t)]$ at time $t$ by the heterogeneous adsorbent for a constant pressure experiment is given by

$$F(t) = \int_0^{\infty} f(t) \cdot \lambda(x)\, dx \tag{16}$$

where $f(t)$ is the local fractional uptake at time $t$ by a pore characterized by the property $x$ ($k_L$ or $D$). The function $\lambda(x)$ is the probability density function for the distribution of the property $x$ in the adsorbents

$$\lambda(x) = \frac{a^{(p+1)}}{\Gamma(p+1)} \cdot (x)^p \cdot e^{-ax} \tag{17}$$

$$\int_0^{\infty} \lambda(x)\, dx = 1 \tag{18}$$

where $\Gamma$ is the gamma function. The variables $a$ and $p$ are two adjustable parameters of the gamma distribution. The mean ($\mu$) and the variance ($\sigma$) of the gamma distribution are given by

$$\mu = \frac{(p+1)}{a}; \quad \sigma^2 = \frac{(p+1)}{a^2} \tag{19}$$

One can now integrate Eq. (16) using the local uptake characteristics [$f(t)$] for the FD or LDF model described by Table 1 (constant pressure experiments) in conjunction with Eqs. (17)–(19) to obtain

*FD Model*:

$$F(t) = 1 - \sum_{n=1}^{\infty} \frac{6}{(n\pi)^2} \cdot \left[ \frac{1}{1 + \left(\frac{\mu t}{R^2}\right) n^2 \pi^2 \chi} \right]^{(1/\chi)} \tag{20}$$

*LDF Model*:

$$F(t) = 1 - \left[ \frac{1}{1 + \mu \chi t} \right]^{(1/\chi)} \tag{21}$$

where $\chi$ is defined by $(\sigma/\mu)^2$. The variable $\chi$ is a measure of the degree of heterogeneity of the adsorbent. The adsorbent is homogeneous when $\chi = 0$. Both Eqs. (20) and (21) reduce to the uptake expressions for homogeneous system given in Table 1 under the limit of [$\chi \to 0, \sigma \to 0$].

We compared the average uptakes on the above described heterogeneous adsorbent by the FD and LDF kinetic models. A set of FD uptake curves was generated using different values of $\chi$ and then they were fitted by the LDF model using different $\chi$ and $\mu$ values. Figure 4 shows the results. The function $F(t)$ is plotted against the dimensionless time $\tau (=\mu t)$ for different values of $\chi$. It may be seen that the difference between the uptake curves by FD and LDF model nearly vanish when the degree of adsorbent heterogeneity is moderate to large ($\chi \geq 1$). Even for a small heterogeneity ($\chi = 0.25$), the difference between the two models is much less than that in the case of a homogeneous adsorbent (Fig. 1). An interesting characteristic of the LDF uptake curves of Fig. 4 is that they intersect the FD uptake curves at two different points.

Figure 5 shows the dimensionless distribution functions [$\lambda(x)$ against $(x/\mu)$] for the three cases shown in Fig. 4. It may be seen that the FD and LDF models show remarkably comparable uptake curves for a heterogeneous adsorbent having a large variety of symmetric and asymmetric distribution characteristics. The homogeneous adsorbent can be described by a Dirac-delta function at $(x/\mu = 1)$ in Fig. 5.

The above example of mass transfer into a heterogeneous adsorbent demonstrates that the detailed characteristics of homogeneous uptake curves (FD or LDF) is not important when the average uptake on a

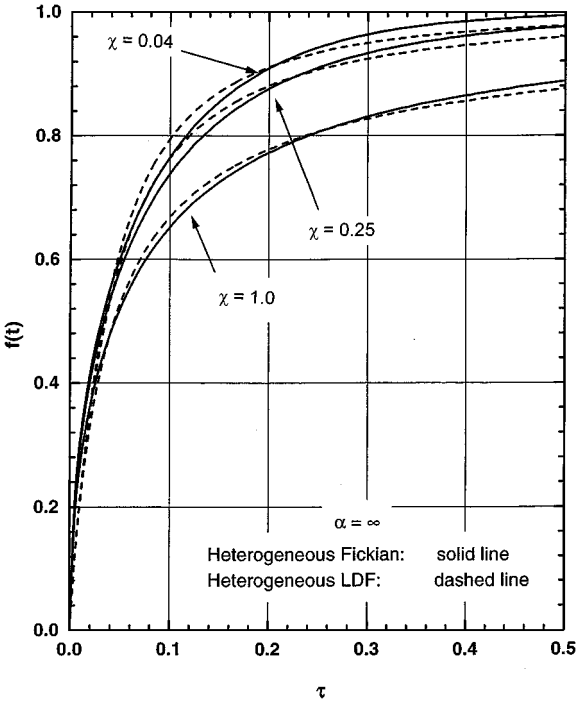


*Figure 4.* Comparative batch kinetic uptakes on model heterogeneous adsorbent by FD and LDF models (constant pressure experiment).

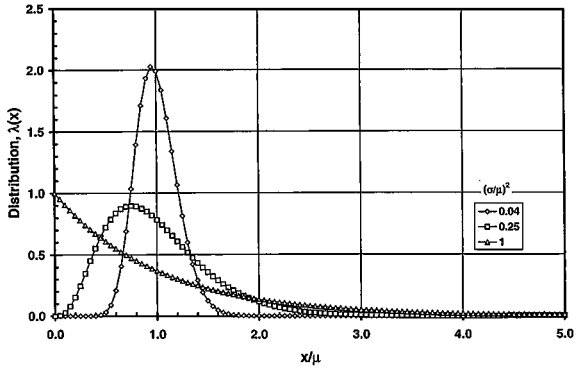


*Figure 5.* Heterogeneity distribution functions corresponding to the cases of Fig. 4.

heterogeneous solid is being estimated. Incidentally, a similar conclusion was reached (Sircar and Myers, 1988) in the past, when describing the overall adsorption equilibria on a heterogeneous adsorbent by integrating the independent contributions of adsorption equilibria from a distribution of adsorption sites of various energies (patchwise homogeneous model). The overall experimentally measured adsorption isotherm on the heterogeneous solid could be described by various combination of energy distribution functions and local adsorption isotherms as long as the mean of the energy distributions were the same. Thus, the detailed characteristics of the local adsorption isotherms and the energy distributions were lost due to the averaging process.

**Column Dynamics**

We consider the isothermal and isobaric adsorption of a single trace adsorbate from an inert gas in a clean adsorbent column at pressure $P$ and temperature $T$. The column is initially pressurized with the pure inert gas at $P$ and $T$. The feed gas having an adsorbate mole fraction of $y^0(\ll 1)$ is then introduced into the column. A single mass transfer zone (MTZ) is formed which propagates through the column as more feed gas is passed and finally the zone exits the column (breakthrough curve) when the column is equilibrated (adsorbate loading $= n^0$) with the adsorbate at feed gas conditions ($P$, $T$, and $y^0$). We assume that the equilibrium adsorption isotherm for the adsorbate is described by the Langmuir model

$$n^0 = \frac{mbPy^0}{1 + bPy^0} \tag{22}$$

where $b$ is the Langmuirian gas-solid interaction parameter for the adsorbate at $T$ and $m$ is the saturation adsorption capacity of the adsorbate.

We further assume that a constant pattern MTZ is formed (Sircar and Kumar, 1983) which dictates that

$$\frac{n(1-y)}{y} = \frac{n^0(1-y^0)}{y^0} \tag{23}$$

where $n$ and $y$ are, respectively, the adsorbate loading and the gas phase adsorbate mole fraction at any position $z$ within the MTZ at any time $t$.

The local rates of adsorption given by Eqs. (1) and (9), respectively, for the LDF and the QDF models can be combined with Eqs. (22) and (23) to obtain the gas phase adsorbate concentration profiles in the breakthrough curves from the column:

*LDF Model*:

$$k_{\mathrm{L}}\frac{(1+bP)}{bP}(t_1 - t_2) = \frac{(1-\theta^0)}{\theta^0}\ln\frac{\phi}{(1-\phi)} - \frac{1}{\theta^0}\ln\left[\frac{1-\phi}{\phi}\right] \tag{24}$$

*QDF Model*:

$$k_{\mathrm{Q}}\frac{(1+bP)}{bP}(t_1 - t_2) = \frac{2(1-\theta^0)}{(2-\theta^0)}\cdot\frac{(1-\theta^0)}{\theta^0}\ln\frac{\phi}{(1-\phi)} - \frac{1}{\theta^0}\ln\left[\frac{1-\phi}{\phi}\right] - \frac{1}{(2-\theta^0)}\ln\left[\frac{2-(1-\phi)\theta^0}{2-(\phi)\theta^0}\right] \tag{25}$$

where $\phi(=y/y^0)$ is the dimensionless gas phase adsorbate concentration, $t_1$ and $t_2$ are, respectively, the times at which the effluent gas dimensionless concentrations are $\phi$ and $(1-\phi)$, and $\theta^0(=n^0/m)$ is the equilibrium fractional surface coverage by the adsorbate at feed gas conditions.

Figure 6 shows three examples of dimensionless column breakthrough curves for $\theta^0$ values of 0.039, 0.181, and 0.997. The variable $\phi$ is plotted against a dimensionless time defined by $[k(1+bP)/(bp)][t-t_s]$ where $t_s$ is the time at which $\phi = 0.5$ [stoichiometric breakthrough time ($t^s = \frac{n^0}{G^0 y^0}$) for the case of

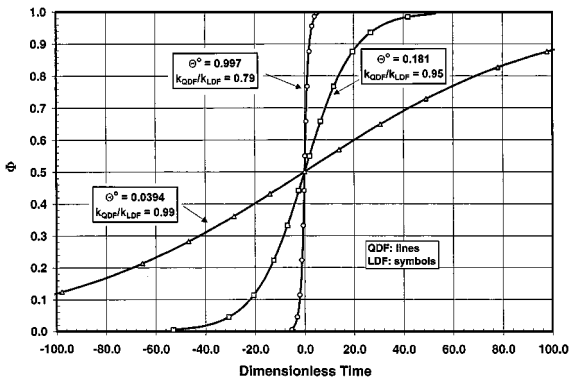


*Figure 6.* Comparative column breakthrough curves by LDF and QDF models.

infinitely fast adsorption of a trace adsorbate, $k_L \to \infty$; $k_Q \to \infty$]. The variable $G^0$ is the molar flow rate of the feed gas per unit amount of adsorbent. The plots of Fig. 6 (symbols) were generated using Eq. (24). They were then refitted (solid lines) by Eq. (25). The results show that the breakthrough curves can be described almost quantitatively by either the LDF or the QDF models for local adsorption kinetics. The ratios of the mass transfer coefficients for the two models ($k_Q/k_L$) for the best fit are given in Fig. 6. This exercise demonstrates that the individual characteristics of batch adsorption kinetics by LDF and QDF (used as a proxy for the FD model) models are lost in describing the column breakthrough curve by the above described integration process.

## Isothermal PSA on a Single Adsorbent Particle

The appropriate relationship between $k_L$ and $(D/R^2)$ that can be used for the design of a PSA process is an often-asked question. In particular, a very interesting situation is the case of a rapid PSA (Sircar et al., 1999) where the cycle times for the adsorption and the desorption steps are very small (<5 seconds). In that case, the adsorbate may only partially penetrate into the mass of the adsorbent particle causing a very inefficient utilization of its total adsorption capacity. However, the overall separation performance by the process can be beneficial (very low adsorbent inventory) due to rapid cycling (Sircar and Hanley, 1995). In such a case, a special relationship [$\Omega_L \gg 10$–16] is needed for process design.

Nakao and Suzuki (1983) numerically studied the separation of a gas mixture (single adsorbate from an inert gas) by an isothermal PSA process over a single adsorbent particle. The adsorption step was carried out by contacting the adsorbent with the gas mixture at a pressure of $P_A$ for a period of time ($t_A$), and then the adsorbate was desorbed by exposing the adsorbent to a lower pressure of $P_D(=0)$ for a period of time ($t_D$). The cyclic process was continued until a steady state was reached. The performance of the process was estimated by using both the FD and the LDF models for adsorption kinetics and a relationship was obtained between $k_L$ and $(D/R^2)$ in order to match the separation efficiency (same amounts adsorbed and desorbed by both models at steady state). The dotted line in Fig. 7 shows the best fit value of $\Omega_L$ as a function of dimensionless cycle time $[D\bar{t}/R^2]$ for the process. The half cycle time for the process is given by $\bar{t}(=t_A = t_D)$.

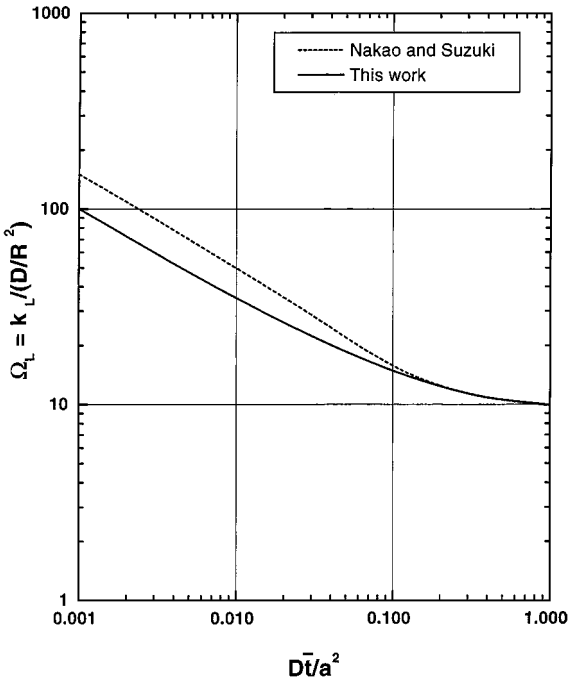


*Figure 7.* Relationship between $k_L$ and $(D/R^2)$ for an ideal PSA process on a single adsorbent pellet. Effect of cycle time.

Recently, it was shown that the ratio of the net effective working capacity for the adsorbate $(\bar{n}_A - \bar{n}_D)$ to the maximum working capacity for the adsorbate $(\bar{n}^*_A - \bar{n}^*_D)$ obtainable under local equilibrium condition for the above described process can be given by (Sircar and Hanley, 1995)

$$\varepsilon = \frac{f_A \cdot f_D}{(f_A + f_D - f_A \cdot f_D)} \tag{26}$$

where $\bar{n}_A$ and $\bar{n}_D$ are the average adsorbate loadings in the particle at the end of, respectively, the adsorption and the desorption steps of the cycle. The variables $\bar{n}^*_A$ and $\bar{n}^*_D$ are, respectively, the equilibrium adsorbate loadings under the conditions of adsorption and desorption. The functions $f_A$ and $f_D$ are, respectively, the fractional uptake (loss) of the adsorbate by the adsorbent during the adsorption and desorption steps:

$$f_A(t_A) = \left[\frac{\bar{n}_A - \bar{n}_D}{\bar{n}^*_A - \bar{n}_D}\right]; \quad f_D(t_D) = \left[\frac{\bar{n}_D - \bar{n}_A}{\bar{n}^*_D - \bar{n}_A}\right] \tag{27}$$

For the special case where $t_A = t_D = \bar{t}$, it follows that $(f_A = f_D = f)$, and:

$$\varepsilon = \frac{f}{(2 - f)} \tag{28}$$

We used Eq. (28) and the constant pressure fractional uptake expressions for LDF and QDF models (Table 1) to obtain a relationship between $k_L$ and $k_Q$ in order to match $\varepsilon$ for the case where $\beta \to 0$. In other words, the conditions of the PSA process were such that the average adsorbate loading in the adsorbent at the start of the adsorption was very small. This condition is expected to be satisfied when $\bar{t}$ is very small so that the adsorbate penetration in the particle is small. The previously obtained best fit relationship between the FD and QDF models [$\Omega_Q = 9.14$] for $\beta = 0$ was then used to obtain $\Omega_L$ as a function of $(D\bar{t}/R^2)$ in order to match the $\varepsilon$ values for the LDF and the FD models. Thus, the QDF model was again used as a proxy for the FD model.

The result is shown by the solid line in Fig. 7. The variable $\Omega_L$ increases as $\bar{t}$ decreases as in the case of Nakao-Suzuki model. In fact, the general agreement between the two results, which were obtained by two completely different approaches and criteria for comparing separation performance, is remarkable. This demonstrates the insensitivity of the choice of adsorption kinetics model in describing process performance. Several authors have developed correlations between $\Omega_L$ and $\bar{t}$ by analysis of various isothermal PSA processes using a single adsorbent particle (Alpay and Scott, 1991; Carta, 1993) as well as a packed column (Raghavan et al., 1986). These studies show that the LDF model can be adequately used to describe the process performance exhibited by the FD model. However, the value of $\Omega_L$ depends on the design of the process.

## Experimental Evidence of LDF Mechanism

The above discussions imply that the CPDF or FD models of gas transport in adsorbent particles provide a more realistic mechanism, but the LDF model can be used as a practical tool for describing the adsorption kinetics on heterogeneous solids, for evaluating adsorbent column dynamics, and for adsorptive process design. It should be mentioned here that the uptake of gases by carbon molecular sieves (CMS), where the primary transport resistance occurs at the restricted pore mouths of the carbon, can be exactly described by the LDF model. Recent experimental uptake data for adsorption of small molecules on CMS measured by the isothermal isotope exchange technique (Rynders et al., 1997) demonstrates that point. It has also been shown that the non-isothermal LDF model can describe gas uptake on zeolites as well as the non-isothermal FD model under the conditions of differential adsorption tests (Sircar, 1983).

## Summary

The Fickian Diffusion (FD) model, which is a special case of the most rigorous chemical potential driving force (CPDF) model of adsorbate transport within an adsorbent particle, is often used for analyzing isothermal gas uptake by adsorbents in order to estimate a diffusivity parameter. The Linear Driving Force (LDF) model with a lumped mass transfer coefficient, on the other hand, is very frequently used for practical analysis of column dynamic data and for adsorptive process design because it is simple, analytical, and physically consistent. Even though the characteristics of the isothermal batch kinetic uptake of a gas by these two models are substantially different, the LDF model works because the estimation of the separation performance of an adsorptive process requires several sets of averaging of kinetic properties at the particle, the column, and the overall cyclic steady state levels. The characteristics of the models describing the local rates of adsorption at the particle level are often lost during these integration processes. This work demonstrates by using simple model systems that (a) the overall fractional uptake by a heterogeneous porous adsorbent, consisting of a collection of parallel pores, can be well described by both the FD or the LDF models characterizing the gas transport into individual pores, (b) the packed-column breakthrough curve for adsorption of a single adsorbate from an inert gas can be well described by both the FD and the LDF models representing adsorption kinetics at the particle level, and (c) the separation efficiency of a simple PSA cycle on a single adsorbent particle is insensitive to the choice of mechanism for the local rates of adsorption. The Quadratic Driving Force (QDF) model is used as a proxy for the FD model in some of these cases.

## Nomenclature

| | |
|---|---|
| $a$ | Parameter of gamma distribution function |
| $b$ | Langmuirian gas-solid interaction parameter |
| $b(t)$ | Function defined by Eq. (11) |
| $B$ | Adsorbate mobility within adsorbent particle |
| $C$ | Adsorbate concentration within adsorbent particle |
| $D$ | Fickian diffusivity of adsorbate within adsorbent particle |

| | |
|---|---|
| $D^0$ | Fickian diffusivity in Henry's Law region |
| $f(t)$ | Fractional uptake at time $t$ |
| $F(t)$ | Fractional uptake at time $t$ on a heterogeneous adsorbent |
| $F(r)$ | Function in Eq. (10) |
| $F_R$ | Value of $F(r)$ at $r = R$ |
| $G_R$ | Function defined by Eq. (12) |
| $H_R$ | Value of $(df/dr)$ at $r = R$ |
| $J$ | Flux of adsorbate inside adsorbent particle |
| $k_{\mathrm{L}}$ | Mass transfer coefficient for LDF model |
| $k_{\mathrm{Q}}$ | Mass transfer coefficient for QDF model |
| $m$ | Langmuirian saturation capacity |
| $n$ | Adsorbate loading in adsorbent particle |
| $n^0$ | Equilibrium adsorbate loading at feed conditions |
| $p$ | Parameter of gamma distribution function |
| $P$ | Pressure |
| $P^{**}$ | Initial pressure change in volumetric experiment |
| $q_{\mathrm{n}}$ | Parameter defined by Table 1 |
| $r$ | Radius |
| $R$ | Radius of adsorbent particle |
| $t$ | time |
| $\bar{t}$ | Half cycle time |
| $T$ | Temperature |
| $y$ | Gas composition |
| $y^0$ | Feed gas composition |
| $x$ | $k_{\mathrm{L}}$ or $D$ as in Eq. (16) |
| $z$ | Distance in column |

*Greek Letters*

| | |
|---|---|
| $\alpha$ | Parameter defined by Table 1 |
| $\beta$ | $\bar{C}^0/(\bar{C}^\infty - \bar{C}^0)$ |
| $\sigma$ | Variance of Gamma distribution |
| $\Gamma$ | Gamma function |
| $\delta$ | Defined by Table 1 |
| $\mu$ | Mean of Gamma distribution, chemical potential |
| $\mu^*$ | Standard state chemical potential |
| $\lambda$ | Defined by Eqs. (16) and (17) |
| $\chi$ | $(\sigma/\mu)^2$ |
| $\theta^0$ | Fractional adsorbate capacity at feed condition |
| $\phi$ | $y/y^0$ |
| $\Omega_{\mathrm{Q}}$ | $k_{\mathrm{Q}}/(D/R^2)$ |
| $\Omega_{\mathrm{L}}$ | $k_{\mathrm{L}}/(D/R^2)$ |
| $\varepsilon$ | Defined by Eq. (28) |
| $\tau$ | Dimensionless time $(Dt/R^2, k_{\mathrm{L}}t, k_{\mathrm{Q}}t)$ |
| $\rho_p$ | Adsorbent particle density |

*Subscripts and Superscripts*

| | |
|---|---|
| 0 | Initial condition |
| $\infty$ | Final condition |
| $*$ | Equilibrium condition |
| $\bar{}$ | Average value in adsorbent particle |
| A | Adsorption |
| D | Desorption |

## References


Alpay, E. and D.M. Scott, "The Linear Driving Force Model for Fast Cycle Adsorption and Desorption in a Spherical Particle," *Chem. Eng. Sci*., **47**, 499–502 (1992).

Barrer, R.M., "Intracrystalline Diffusion," in *Adv. in Chemistry Ser*., Vol. 102, R.F. Gould (Ed.), p. 1, ACS, 1971.

Buzanowski, M.A. and R.T. Yang, "Approximations for Intraparticle Diffusion Rates in Cyclic Adsorption and Desorption," *Chem. Eng. Sci*., **46**, 2589–2598 (1991).

Carta, G., "The Linear Driving Force Approximation for Cyclic Mass Transfer in Spherical Particles," *Chem. Eng. Sci*., **48**, 622–625 (1993).

Chihara, K. and M. Suzuki, "Simulation of Nonisothermal Pressure Swing Adsorption," *J. Chem. Eng. Japan*, **16**, 53–61 (1983).

Crank, J., *Mathematics of Diffusion*, Oxford University Press, London, 1956.

Do, D.D. and P.L.J. Mayfield, "A New Simplified Model for Adsorption in a Single Particle," *AIChE J*., **33**, 1397–1400 (1987).

Do, D.D. and R.G. Rice, "Validity of the Parabolic Profile Assumption in a Single Particle," *AIChE J*., **32**, 149–154 (1986).

Gemmingen, U.V., "Pressure Swing Adsorption Process—Design and Simulations," in *Proceedings of IVth Int. Conf. on Fundamentals of Adsorption*, Kyoto, Kodansha, Japan, 1993, M. Suzuki (Ed.), pp. 703–712.

Gleuckauf, E., "Theory of Chromatography Part 10: Formula for Diffusion into Spheres and Their Applications in Chromatography," *Trans. Faraday Soc*., **51**, 1540–1551 (1955).

Gleuckauf, E. and J.I. Coates, "The Influence of Incomplete Equilibrium on the Front Boundary of Chromatograms and the Effectiveness of Separation," *J. Chem. Soc*., 1315–1321 (1947).

Goto, M. and T. Hirose, "Modified Parabolic Profile Approximation of Intraparticle Concentration for Chemical Reaction and Adsorption," *J. Chem. Eng. Japan*, **24**, 538–542 (1991).

Hartzog, D.G. and S. Sircar, "Sensitivity of PSA Process Performance to Input Variables," *Adsorption*, **1**, 133 (1995).

Karger, J. and D.M. Ruthven, *Diffusion in Zeolites*, Wiley-Interscience, New York, 1992.

Liaw, C.H., J.S.P. Wang, R.A. Greenkorn, and K.C. Chao, "Kinetics of Fixed Bed Adsorption: A New Solution," *AIChE J*., **25**, 376–381 (1979).

Mohr, R.J., D. Vorkapic, M.B. Rao, and S. Sircar, "Pure and Binary Gas Adsorption Equilibria and Kinetics of Methane and Nitrogen on 4A Zeolite by Isotope Exchange Technique," *Adsorption*, **5**, 145–158 (1999).

Nakao, S. and M. Suzuki, "Mass Transfer Coefficient in Cyclic Adsorption and Desorption," *J. Chem. Eng. Japan*, **16**, 114–119 (1983).

Raghavan, N.S., M.M. Hassan, and D.M. Ruthven, "Numerical Simulation of a PSA System Using a Pore Diffusion Model," *Chem. Eng. Sci*., **41**, 2787–2793 (1986).

Ruthven, D.M., *Principles of Adsorption and Adsorption Processes*, John Wiley and Sons, New York, 1984.

Ruthven, D.M., L.K. Lee, and J. Yucel, "Kinetics of Non Isothermal Sorption in Molecular Sieve Crystals," *AIChE J*., **26**, 16–23 (1980).

Rynders, R.M., M.B. Rao, and S. Sircar, "Isotope Exchange Technique for Measurement of Gas Adsorption Equilibria and Kinetics," *AIChE J*., **43**, 2456–2470 (1997).

Sircar, S., "Linear Driving Force Model for Non-Isothermal Gas Adsorption Kinetics," *J. Chem. Soc. Faraday Trans. I*., **79**, 785–796 (1983).

Sircar, S. and B.F. Hanley, "Production of Oxygen Enriched Air by Rapid Pressure Swing Adsorption," *Adsorption*, **1**, 313–320 (1995).

Sircar, S. and J.R. Hufton, "Intraparticle Adsorbate Concentration Profile for Linear Driving Force Model," *AIChE J*., **46**, 659–660 (2000).

Sircar, S. and R. Kumar, "Adiabatic Adsorption of Bulk Binary Gas Mixtures: Analysis by Constant Pattern Model," *Ind. Eng. Chem. Process. Des. Dev*., **22**, 271–280 (1983).

Sircar, S. and A.L. Myers, "Equilibrium Adsorption of Gases and Liquids on Heterogeneous Adsorbents—A Practical Viewpoint," *Surface Science*, **205**, 353–386 (1988).

Sircar, S., M.B. Rao, and T.C. Golden, "Fractionation of Air by Zeolites," in *Adsorption and Its Applications in Industry and Environmental Protection*, Vol. 1, A. Dabrowski (Ed.), pp. 395–423, Elsevier, 1999.

Vermeulen, T., "Theory for Irreversible and Constant Pattern Solid Diffusion," *Ind. Eng. Chem*., **45**, 1664–1670 (1953).

Yao, C. and C. Tien, "Approximation of Intraparticle Mass Transfer in Adsorption Processes—Linear Systems," *Chem. Eng. Sci*., **47**, 457–464 (1992a).

Yao, C. and C. Tien, "Approximation of Intraparticle Mass Transfer in Adsorption Processes—Non-Linear Systems," *Chem. Eng. Sci*., **47**, 465–473 (1992b).

Yucel, H. and D.M. Ruthven, "Diffusion in 5A Zeolite—Study of the Effect of Crystal Size," *J. Chem. Soc. Faraday Trans. I*, **76**, 71–83 (1980).